



# Quality Control for Second-Level Radiosonde Data Based on Bezier Curve Fitting

Huixia Lai<sup>1,\*</sup>, Lian Chen<sup>1,\*</sup>, Hualin Zhang<sup>2</sup>, Ye Tian<sup>4</sup>, Weijie Zhang<sup>1</sup>, Bo Wang<sup>2</sup>, and Shi Zhang<sup>1,3</sup>

<sup>1</sup>the College of Computer and Cyber Security, Fujian Normal University, Fuzhou, China

<sup>2</sup>Fujian Meteorological Information Center, Fuzhou, China

<sup>3</sup>the Digit Fujian Internet-of-Things Laboratory of Environmental Monitoring, Fujian Normal University, Fuzhou, China

<sup>4</sup>Beijing Municipal Meteorological Observation Center, Beijing, China

\*These authors contributed equally to this work.

**Correspondence:** Bo Wang (66623421@qq.com) and Shi Zhang (shi@fjnu.edu.cn)

**Abstract.** The balloon-borne radiosonde observations provide high-resolution profile observations of pressure, temperature, relative humidity, and winds from the surface to the middle stratosphere. These observations help validate space-based data and are used in climate research, weather forecasting. For the large amount of second-level radiosonde data, it is tedious and time-consuming for the manual quality control (QC). Furthermore, varying experiences and different judgment standards may lead to inconsistent judgments for abnormal data. To address these issues, we propose a two-stage QC method for second-level radiosonde data based on the Bezier curve fitting. In the stage QC1, the gross errors are filtered out according to the measurement range of the sensors, the change rates and extreme temperature values based on pressure segmentations. Also, the algorithm of the longest descending sequence(LDS) is used to identify the moment of sounding termination and eliminate items after that moment. In the stage QC2, we score each item with deviations calculated using Bezier curve fitting, and then use a decision tree model ,CART, to identify anomalies in second-level radiosonde data. The experiment results first demonstrate the efficacy of QC at each step, and finally validate the rationality of our method by comparing the statistical characteristics before and after QC. After QC, the error items are greatly reduced, and the percentile profile distribution of temperature, pressure and relative humidity becomes more reasonable. The overlap of items identified by manual QC and automatic QC reaches 86%, verifying the effectiveness of our method. This research significantly boosts QC efficiency and unifies the QC standards, providing quality assurance for various applications.

## 1 Introduction

Upper-air meteorological observation is an important means of understanding the atmosphere. The observation instrument includes satellite, aircraft, radar, radiosonde, etc. (Guo et al., 2020). Among them, the balloon-borne radiosonde system combines radar and radiosonde carried by balloon for upper-air meteorological observation, which is one of the main direct detection methods and can obtain vertical distribution data such as atmospheric temperature, pressure, and humidity (Houchi et al., 2015; Agarwal and Sun, 2021; Cao et al., 2019).



China Meteorological Administration (CMA) takes upper air observations with radiosondes (as shown in Figure 1). As the radiosonde rises at about 6 meters/second, sensors in the radiosonde radio pressure, temperature, relative humidity (radiosonde data) back to a ground station every 1.2 seconds. Wind speed and direction aloft (rawinsonde data) are also obtained by tracking the position of the radiosonde in flight using L-band radar. The L-band second-level up-air sounding data, including radiosonde data and rawinsonde data, provides high vertical resolution flight data for numerical weather forecasting, climate analysis, scientific research, and international exchange (Faccani et al., 2009; Kumar and Sunilkumar, 2020; Zhang et al., 2024; Tan et al., 2022).

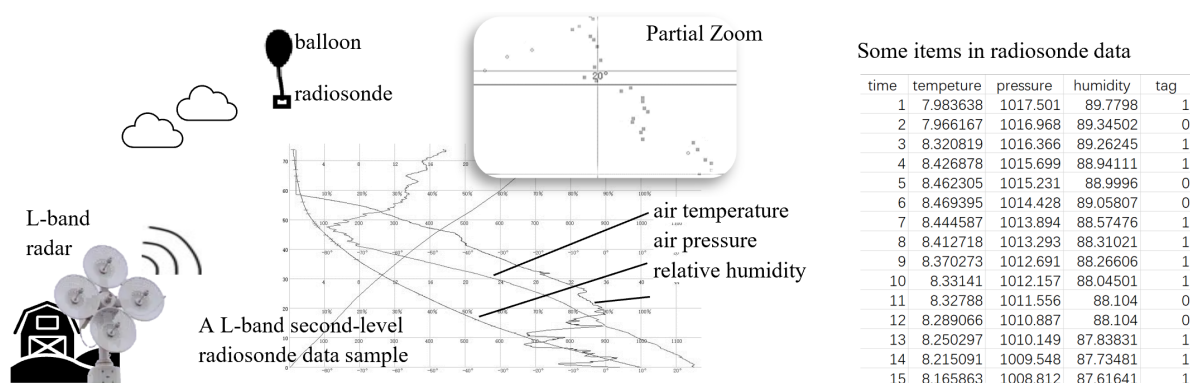


**Figure 1.** Schematic diagram of L-band upper-air sounding observation and some radiosonde data samples.

The balloon-borne radiosonde observation has the advantages of high accuracy, high detection height, and is not affected by weather. Therefore, it plays an irreplaceable role in upper-air meteorological observation. However, affected by various factors such as equipmenfaultslt, communication failure, and severe weather, the radiosonde data often contains a lot of unrealistic observations (outliers, errors, or anomalies). In the fields of climate research and meteorological forecasting, the impact of these erroneous values can be propagated and amplified, seriously affecting the effectiveness of data application (Estévez et al., 2011). Therefore, it is an important task to eliminate these anomalies before applying (Zhai, 1997; Guo et al., 2009).

In 2010, CMA released an operational specification, "Operational specification for routine upper air meteorological observation", to guide the data processing (meteorological administration, 2010). The specification does not propose quantitative criteria for filtering out abnormalities, only provides some guiding opinions. At present, the quality control (QC) of second-level radiosonde data mainly relies on manual screening. Due to lack of quantized criteria and different experience for each personnel, manual QC on the radiosonde data is not only tedious and time-consuming, but also often leads to inconsistent decisions regarding abnormalities by quality control personnel. These issues highlight the limitations of manual QC. Therefore, there is an urgent need for a more efficient and standardized method to improve QC efficiency, and unify QC standards.

The classic quality control methods for up-air sounding data focus on statistical methods, which include extreme value analysis, consistency analysis, wind shear analysis, and static analysis (Durre et al., 2008; Graybeal et al., 2004; Chen and Xu, 2018; Houchi et al., 2010, 2015). Recently, researchers proposed more complicated methods for the quality control of up-air sounding data, such as the improved statics analysis proposed by Xiong (Xiong, 2015), temperature super adiabatic



decline rate analysis, double weight outlier analysis, and balloon acceleration analysis by Wang (Wang et al., 2020, 2022). Agarwal (Agarwal and Sun, 2021) proposed a set of robust quantile methods to characterize the distribution as well as an outlier detection procedure to identify both magnitude and shape outliers. Although the above methods improved the quality of temperature, pressure, relative humidity (RH) in sounding data, they mainly focused on the quality control of rawinsonde data (Graybeal et al., 2004; Houchi et al., 2010, 2015; Agarwal and Sun, 2021). Hao (Hao et al., 2020) and Wang (Wang et al., 2022) pointed out that the deviation of RH and temperature was mainly limited by sensors. Considering that anomaly detection on RH and temperature is complex and largely depends on the improvement of sensors, their researches also focused more on rawinsonde data.

The radiosonde data is widely used in many studies but with limited references to QC aspects. Qian (Qian et al., 2019) used pattern validation to evaluate the quality of temperature series; Wang (Wang et al., 2022) conducted extreme value checks on temperature and pressure. However, these methods just focused on the statistical characteristics of historical data to realize data quality control. They can only eliminate obvious abnormalities and do not fully utilize the characteristics of 3 meteorological observation variables (pressure, temperature, and relative humidity), such as the continuity of temperature changes and the monotonically decreasing pressure, to carry out further quality control on radiosonde data.

In this paper, we propose a two-stage quality control method based on Bezier curve fitting for second-level radiosonde data. In the first stage (QC1), gross errors are screened out. In the second stage (QC2), some random errors, systematic errors, and micro meteorological errors are filtered out. By comparing the statistical characteristics of historical data from Fuzhou sounding station before and after automatic QC, the feasibility of our method was verified. (1) After quality control, errors are significantly reduced, and the percentile profiles of temperature, pressure, and relative humidity are more reasonable. (2) The overlap ratio between automatic QC results and manual QC results reaches 86%, indicating that our method can accurately detect errors in radiosonde data. Compared with manual QC, the method proposed in this paper can not only significantly reduce the human resource cost, but also help unify the QC standards of radiosonde data, effectively improving the reliability and accuracy of data quality control. This study provides a new attempt at quality control of continuous meteorological data.

## 2 Datasets

### 2.1 Data description

The second-level radiosonde dataset comes from Fujian Meteorological Information Center. The dataset is collected by L-band (Type-I) radiosonde system at Fuzhou National Balloon Sounding Station. The station carries out routine up-air meteorological sounding observations at 08:00 and at 20:00 LT every day using an operational L-band radiosonde system (Guo et al., 2016). The radiosonde dataset used in this paper includes observation results from January 1, 2020 to December 31, 2022, with a total of 2275 effective balloon-borne sounding. During this period, an average of 4069 items were obtained for each upper-air sounding. Each item consists of time, temperature, pressure, and relative humidity. Among these items, an average of 782 items were filtered out by manual quality control for each upper-air sounding result, accounting for 19.2%. This dataset provides a rich data source to evaluate and validate the proposed quality control methods.



## 2.2 Data analysis

80 Based on the dataset, the statistical characteristics of temperature, pressure, and relative humidity from height-segmented radiosonde data are shown in Figure 2. It can be seen that the ranges of temperature, pressure, and relative humidity at different heights show a wide span. For example, within 1000 meters, the temperature ranges from  $+50^{\circ}\text{C}$  to  $-90^{\circ}\text{C}$ , which is inconsistent with the latitude and climate of Fuzhou city. The data dispersion indicates that second-level radiosonde data often contains many anomalies (errors). The existence of such abnormalities poses challenges for subsequent data analysis and appli-  
85 cation. Therefore, effective data quality control is necessary to ensure the data reliability and the correctness of meteorological analysis.

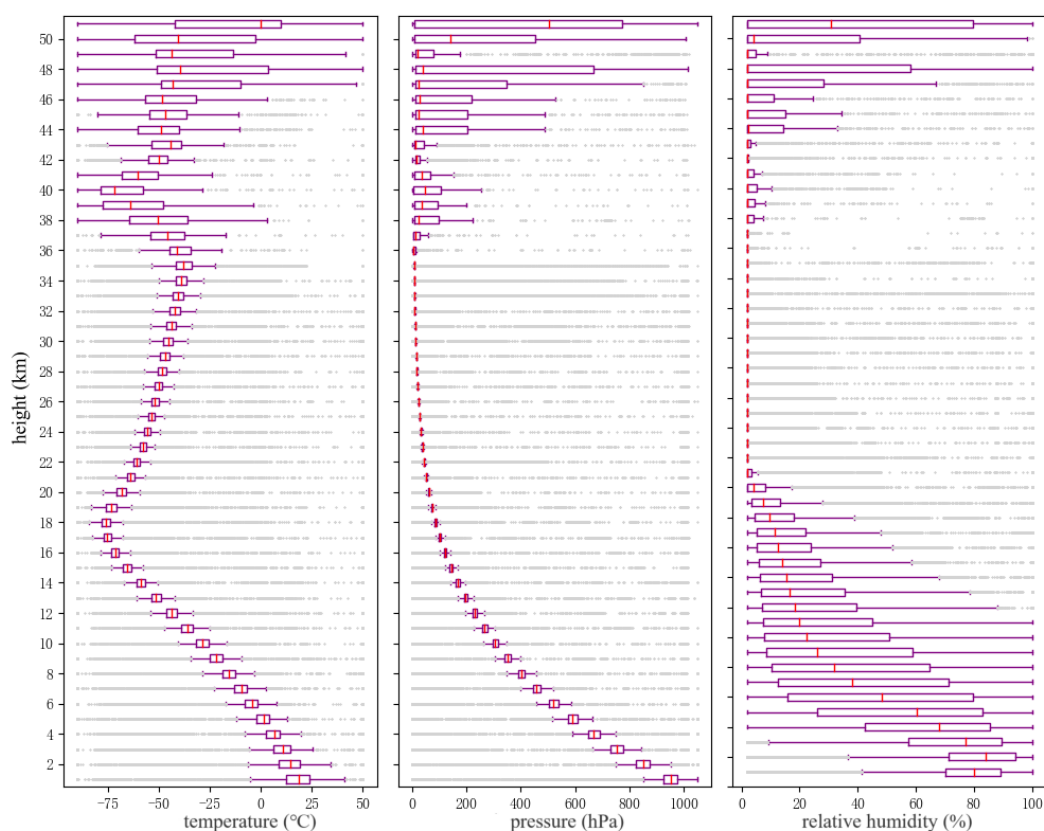


**Figure 2.** Statistical characteristics of temperature, pressure, and relative humidity from height-segmented radiosonde data (January 1,2020 ~ December 31, 2022).

The dataset used in this paper includes labels marked by QC personnel. However, by examining this data, we find that there are many inconsistencies in quality control criteria conducted by different QC personnel. The same situations also exist in different QC processes done by the same quality control personnel. For example, from the two sub-series of temperature  
90 displayed by the L-band (Type-I) data processing software (Figure 3(a, b)), filtered out points reveal inconsistent standards



when the relative humidity and pressure are normal. In Figure 3(a), comparing between ① and ②, ① is more like an anomaly than ② in the overall trend, but ② is misjudged as an anomaly. In Figure 3(b), the cases of ⑤ and ⑥ demonstrate inconsistent data processing for continuous invariant temperatures, where 3 temperatures in ⑥ are filtered out while all temperatures in ⑤ are retained. Similar inconsistent situations are also reflected in the comparison of ③, ④, and ⑦ in Figure 3(b). In addition, there are also omissions in the manual quality control, as shown in Figure 2 (c) where a pressure outlier is not labeled.

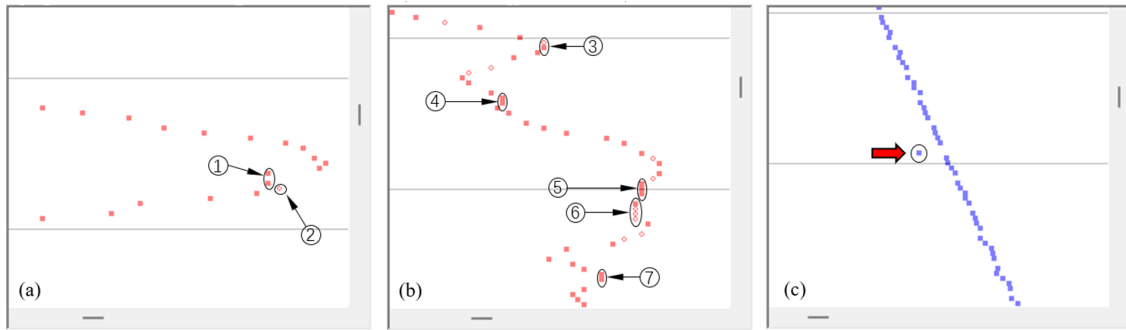


**Figure 3.** Three data sub-series are displayed using L-band (Type I) data processing software. (a) Temperature sub-series from 58:02 to 58:24, sounding at 08:00, Jan.28,2020; (b) Temperature sub-series from 67:30 to 68:37, sounding at 08:00, Jan.28,2020; (c) Temperature sub-series with a neglected anomaly temperature at 67:02, sounding at 08:00, Jun.15,2020.

These examples indicate that inconsistencies and omissions in manual QC may affect the effectiveness of quality control, thereby affecting the availability and reliability of the final data. So, developing an automated quality control system is important to ensure consistency and accuracy in radiosonde data processing.

### 100 3 A quality control method based-on Bezier curve fitting

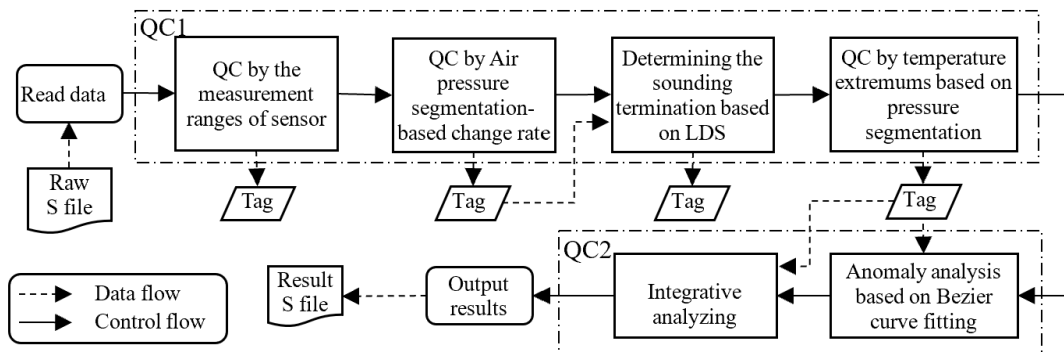


**Figure 4.** The workflow of quality control method based-on Bezier curve fitting for second-level radiosonde data.



The errors / anomalies in meteorological data can be classified into four categories: random errors, systematic errors, micrometeorological (representative) errors, and gross errors (Wang et al., 2007; Zahumensky, 2004; Estévez et al., 2011). In response to these errors, we propose a quality control method for second-level radiosonde data based on Bezier curve fitting. The workflow of our method is shown as Figure 4. In stage QC1, first, the preliminary quality control, including QC on the measurement ranges of sensors and the pressure-segmentation-based change rates of the 3 meteorological variables (temperature, pressure, relative humidity), is carried out. The two steps aim to quickly filter out obvious errors. Next, the algorithm, the longest decreasing sub-sequence (LDS) of pressure, is used to identify the moment of sounding termination. It helps to eliminate invalid items generated after the balloon burst. Finally, we further filter out the anomalies by the pressure segmentation-based temperature extremums. In the stage QC2, it goes further by first fitting the output data of QC1 with a Bezier curve to obtain a deviation sequence, then analyzing the deviations, and finally calculating the anomaly scores for each item. Afterwards, a machine learning method is used to classify the second-level radiosonde data. The adaptability of our method to various error types is shown in Table 1.

**Table 1.** The adaptability of our method to various types of error (✓: solved; ✗: partially solved).

Error type	Random error	Systematical error	Micrometeorological error	Gross error
QC1				✗
QC2	✗	✗	✗	✗
QC1+QC2	✗	✗	✗	✓

For ease of description, we first define variables used in this paper. By parsing the raw data file (referred to as S files), we obtain time, temperature, pressure, and relative humidity sequences. They are represented by  $Time_{1..n}$ ,  $T_{1..n}$ ,  $P_{1..n}$  and  $H_{1..n}$ , where  $n$  is the sequence length. The temperature ( $t_g$ ), pressure ( $p_g$ ), and relative humidity ( $h_g$ ) on the ground can also be read from the S file. In addition, we set a sequence  $Tag$  with initial values of 0 to store the judgment result. In the quality control processing, if the  $i$ -th item is abnormal, we set  $Tag_i$  to 1. The sequence  $B$  is set up to store the fitting values of the Bezier curve.

To unified processing the first and the last points,  $Time_{1..n}$ ,  $T_{1..n}$ ,  $P_{1..n}$  and  $H_{1..n}$  are extended to  $Time_{0..n+1}$ ,  $T_{0..n+1}$ ,  $P_{0..n+1}$  and  $H_{0..n+1}$ . We initialize the extended items as follows:

$$Time_0 = 2Time_1 - Time_2, Time_{n+1} = 2Time_n - Time_{n-1};$$

$$T_0 = t_g, T_{n+1} = T_n + (T_n - T_{n-1});$$

$$P_0 = p_g, P_{n+1} = P_n + (P_n - P_{n-1});$$

$$H_0 = h_g, H_{n+1} = H_n + (H_n - H_{n-1}).$$



### 125 3.1 Quality Control in stage QC1

In stage QC1, the first step, quality control according to the measurement ranges of temperature, pressure, and relative humidity sensors, can quickly eliminate errors that exceed the physical measurement ranges of the sensor. This step is simple and easy to implement. Therefore, in the rest of this subsection, we mainly describe the other three QC steps.

#### 3.1.1 QC by the pressure segmentation-based change rates

130 Pressure segmentation-based change rates are statistics of historical labeled data. These change rates were utilized to identify abnormal items in the current radiosonde data. Taking temperature as an example, the following provides a detailed description of the statistic and the application of historical temperature change rates based on pressure segmentation.

(1) Based on manually labeled historical radiosonde data, calculate the change rates of temperature over time, denoted as  $r_i$ , to obtain the historical change rate set  $R$ . The calculation is as follows:

$$135 R = \{(P_i, r_i) | r_i = \frac{T_i - T_{i-1}}{Time_i - Time_{i-1}} \text{ and } i \in [1..n]\} \quad (1)$$

(2) Group the change rates according to pressure segmentations, and then calculate the maximum and minimum change rates of temperature in each bin. The processing is shown in Formula 2 and Formula 3:

$$T_{MAX} = \{\max(\{r_i | k * step < P_i < (k + 1) * step \text{ and } (P_i, r_i) \in R\}) | k \in \{0, \lfloor \frac{1050}{step} \rfloor\}\} \quad (2)$$

$$140 T_{MIN} = \{\min(\{r_i | k * step < P_i < (k + 1) * step \text{ and } (P_i, r_i) \in R\}) | k \in \{0, \lfloor \frac{1050}{step} \rfloor\}\} \quad (3)$$

where  $k$  is the number of pressure bins, 1050 is the upper limit of the measurement range of the pressure sensor, and  $step$  is the span of each segmentation.

(3) Fit the maximum and minimum change rates of temperature with polynomial. We achieve the functions of the extreme values on temperature based on pressure. The functions are used as the thresholds of the temperature change rate, with the upper and lower bounds denoted as  $maxF(\cdot)$  and  $minF(\cdot)$ .

(4) Let the fitting function of extreme values as thresholds, classify items as normal or abnormal. This step can be denoted as formula 4:

$$Tag_i = \begin{cases} 0 & minF(P_i) \leq r_i \leq maxF(P_i), 1 \leq i \leq n \\ 1 & other \end{cases} \quad (4)$$

Steps (1~3) gather statistics of changing rates ranges on historical labeled radiosonde data. For the first time, steps (1~3) will run on all historical data. In subsequent use, they can be updated incrementally. In step (4), we filter out the anomaly values and set  $Tag[\cdot]$ .





### 3.1.2 QC by the moment of sounding termination based on LDS

After released, the balloon gradually expands in size owing to the decrease in air pressure. When the balloon reaches a diameter of 6 to 8 meters, it bursts. The radiosonde continues to send data after the burst. In order to filter out invalid data collected while the radiosonde descends, it is necessary to identify the moment of sounding termination accurately. During the ascent of the balloon, irregular pressure values may be collected because of turbulence. Therefore, it is inappropriate to simply determine the moment of sounding termination based on the minimum pressure. In this step, we find the moment of sounding termination by searching for the longest decreasing sub-sequence (LDS) of the pressure sequence.

Let  $LDS[\cdot] = 0$ ,  $P[0] = -\infty$  ( $P[0]$  will be recovered after Algorithm 1), where  $LDS[i]$  represents the longest decreasing sub-sequence length ending with the  $i$ -th item of the sequence. The value of  $LDS[i]$  depends on the longest decreasing sub-sequence length of all items that are smaller than it in  $P[0..i-1]$ .  $LDS[i]$  is defined as Formula 5.

$$LDS[i] = \max(\{LDS[k] | P[k] < P[i] \text{ and } k \in [0..i]\}) + 1 \quad (5)$$

where  $i \in [1..n]$ .

The algorithm for finding the moment of sounding termination based on LDS is described as Algorithm 1. The algorithm calculates LDS in lines 01-09 and locates the sounding termination moment  $time_{burst}$  in lines 10-13. According to the sounding termination moment, the items after that moment can be excluded. Therefore, the  $Tag[\cdot]$  can be modified according to Formula 6.

$$Tag_i = \begin{cases} 1 & time_{burst} < Time_i \text{ and } 1 \leq i \leq n \\ Tag_i & \text{others} \end{cases} \quad (6)$$

### 3.1.3 QC by pressure segmentation-based temperature extremums

During the ascent of a balloon, the temperature is not monotonically decreasing. It first decreases as the balloon rises, and then slowly increases in the atmospheric inversion layer. In this QC step, we first construct a mapping from pressure to temperature based on historical data from the same upper-air sounding station, and then abnormal temperature values are filtered out using pressure segmentation-based historical temperature extremums. This step can not only identify anomaly temperature values that deviate significantly from the normal trend and value range during the ascent of balloons, but also discover some special weather processes where the temperature sequence deviates as a whole.

Let  $S$  be a sequence of pairs (pressure, temperature). These data are extracted from historical labeled radiosonde data. The steps for detecting anomalies by temperature extremums based on pressure segmentation are as follows:

- (1) Sort  $S$  non-incrementally based on pressure to obtain an ordered sequence  $S'$ ;
- (2) Divide the ordered sequence  $S'$  into  $m$  groups (as formula 7). Then, determine the temperature extreme values for each pressure segmentation with the  $3\sigma$  principle, as shown in Formula 8 and Formula 9.

$$TGroup_i = \{S'[k].T | k \in [i \times \frac{|S'|}{m}, (i+1) \times \frac{|S'|}{m}]\} \quad (7)$$






---

**Algorithm 1** Determining the moment of sounding termination based on LDS

---

**Require:**  $P$ : pressure array;  $time$ : time array;  $Tag$ : tags outputed from the previous steps.

**Ensure:**  $time_{burst}$ : the moment of sounding termination.

```

1: int  $n = P.size()$ 
2: vector<int>  $LDS(n, 0)$ 
3: for ( $i = 0; i \geq n - 1; ++i$ ) do
4:   for ( $k = 0; k < i + 1$  and  $Tag[i]; ++k$ ) do
5:     if ( $Tag[k] == 0$  and  $P[i] < P[k]$  and  $LDS[i] < LDS[k]$ ) then
6:        $LDS[i] = LDS[k] + 1$ 
7:     end if
8:   end for
9: end for
10: for ( $i = 0, burst = n; LDS[burst] < LDS[i]; --i$ ) do
11:    $burst = i$ 
12: end for
13: return  $time[burst]$ 
    
```

---

$$T_{MAX} = \{\mu(TGroup_k) + 3\sigma(TGroup_k) | 1 \leq k < m\} \quad (8)$$

$$T_{MIN} = \{\mu(TGroup_k) - 3\sigma(TGroup_k) | 1 \leq k < m\} \quad (9)$$

where  $m$  is the number of groups;  $S'[k]$  represents the  $k$ -th group of  $S'$ ,  $S'[k].T$  is the temperature in the pair,  $\mu(TGroup_k)$  and  $\sigma(TGroup_k)$  represent the mean and the standard deviation of temperatures in the  $k$ -th group.

(3) Construct the temperature maximum (minimum) function regarding pressure using inverse distance weighting (IDW) interpolation. The two functions,  $maxFPT(\cdot)$  and  $minFPT(\cdot)$ , output the thresholds for temperature in different pressure values. They are defined as Formula 10 and Formula 11.

$$maxFPT(x) = \frac{\sum_{i=1}^m w_i(x) T_{MAX_i}}{\sum_{i=1}^m w_i(x)} \quad (10)$$

$$minFPT(x) = \frac{\sum_{i=1}^m w_i(x) T_{MIN_i}}{\sum_{i=1}^m w_i(x)} \quad (11)$$

where  $x$  represents the pressure,  $maxFPT(x)$  and  $minFPT(x)$  return the maximal temperature and the minimal temperature of the target point, and the weight  $w_i(x) = \frac{1}{|x-x_i|^2}$  is the reciprocal of the square of the distance between the target point and the  $i$ -th discrete point  $x_i$ .



(4) Use the extreme value as the temperature threshold at different pressures to filter out temperature anomalies, as shown in  
 195 Formula (12).

$$Tag_i = \begin{cases} 0 & \min FPT(P_i) \leq T_i \leq \max FPT(P_i) \text{ and } 1 \leq i \leq n \\ 1 & \text{others} \end{cases} \quad (12)$$

Steps (1~3) gather statistics from historical labelled radiosonde data. In subsequent use, they can be updated incrementally. In step (4), anomalies are filtered out.

### 3.2 Quality Control in stage QC2

200 The quality control of the stage QC1 exclude items with significant deviations and items after the moment of balloon burst. To further improve the data quality, we introduce two steps in the stage QC2: (1) Anomaly analysis based on Bezier curve fitting; (2) Machine learning based integrative judgment. Taking temperature as an example, we explain the process in the following. The same method applies to pressure and relative humidity sequences.

#### 3.2.1 Anomaly analysis based on Bezier curve fitting

205 In the atmosphere, temperature, pressure, and relative humidity are continuous variables. The characteristic of continuous change is crucial for the manual QC. A Bezier curve is a smooth curve that is generated from a sequence of polylines formed by several data points (control points) in space as the contour (Su et al., 2020; Gordon and Riesenfeld, 1974). The smooth Bezier curves reflect the continuous variation characteristics of meteorological variables in the atmosphere. Therefore, we first perform Bezier curve fitting based on control points, and then evaluate the degree of deviation using the difference between the  
 210 fitted value and the observed value.

**The definition of Bezier curve:** Given  $n + 1$  control points  $\{P_k = (p_{k,1}, p_{k,2}, \dots, p_{k,d}) | k = 0, 1, 2, \dots, n\}$ , the Bezier curve of order  $n$  is given by:

$$P(t) = \sum_{k=0}^n P_k \cdot BEZ_{k,n}(t) \quad (13)$$

where  $d$  is the data dimension,  $t$  is a parameter, and  $0 \leq t \leq 1$ , vector  $P_k$  is the control point,  $BEZ_{k,n}(t)$  is a Bezier basis  
 215 function defined by Bernstein polynomial as formula ??.

$$BEZ_{k,n}(t) = C_n^k t^k (1-t)^{n-k} = \frac{n!}{k!(n-k)!} t^k (1-t)^{n-k} \quad (14)$$

The number of control points affects the shape of the curve. Taking the Bezier curve with 3 control points ( $P_0, P_1, P_2$ ) as an example, its parameter equation can be defined as:

$$P(t) = \sum_{k=0}^2 P_k \cdot BEZ_{k,2}(t) = (1-t)^2 P_0 + 2t(1-t)P_1 + t^2 P_2 \quad 0 \leq t \leq 1 \quad (15)$$



220 **Application of Bezier Curve:** Through experiments, we find that high-order Bezier curves are prone to overfitting and may cause instability. The local changes in meteorological variables are more suitable for fitting with 2-order Bezier curves.

Let  $y = (Time_k, T_k)$ , where the  $Time_k$  is time, and the  $T_k$  is temperature. Find the first data  $x = (Time_i, T_i)$  that has not been classified as abnormal before  $k$ , and the first data  $z = (Time_j, T_j)$  that has not been classified as abnormal after  $k$ . Take  $x$ ,  $y$ , and  $z$  as the 3 control points of the Bezier curve.

225 Firstly, calculate the parameter  $t$  using Formula 16.

$$t = \frac{Time_i - Time_k + \sqrt{Time_k^2 - Time_i Time_j + (Time_i - 2Time_k + Time_j)Time_k}}{Time_i - 2Time_k + Time_j} \quad (16)$$

By substituting the calculated  $t$  into Formula 15, the expression for calculating the fitting value of  $T_k$ ,  $T'_k$ , can be defined as:

$$T'_k = \begin{bmatrix} T_i & T_k & T_j \end{bmatrix} \begin{bmatrix} 1 & -2 & 1 \\ 0 & 2 & -2 \\ 0 & 0 & 1 \end{bmatrix} \begin{bmatrix} 1 \\ t \\ t^2 \end{bmatrix} \quad (17)$$

230 The degree of deviation is obtained by dividing the deviation between the fitted value and the actual value,  $T'_k - T_k$ , by the changing rate of the two control points  $\frac{T_j - T_i}{Time_j - Time_i}$ . Finally, we evaluate the anomaly scores for each temperature value in the radiosonde data using the Formula 18.

$$T\_SCORE_i = \left| \frac{2}{1 + e^{\frac{(T'_k - T_k)(Time_j - Time_i)}{T_j - T_i}}} - 1 \right| \quad (18)$$

Similarly, by fitting Bezier curves for pressure and relative humidity, the anomaly scores  $P\_SCORE$  and  $H\_SCORE$  for pressure and relative humidity can be achieved.

### 235 3.2.2 Integrative analyzing

Based on the anomaly scores  $T\_SCORE$ ,  $P\_SCORE$ , and  $H\_SCORE$ , we first utilize CART decision tree (Zhou, 2016) for classifying radiosonde data items. Afterwards, we merge  $Tag$  with the classification results, and realize the quality control on radiosonde data. In the experiments, the CART decision tree adopts the Gini index (criterion="gini") as the criterion for selecting classification features, sets the best segmentation strategy (splitter="best"), sets min\_samples\_leaf to 2, and the  
 240  $max\_depth$  to 7.

## 4 Experiment and discussion

In the experiment, the dataset is divided into training data (2020-2021) and testing data (2022). Our QC method, Bezier Curve fitting-based Quality Control method, needs to be trained with the historical data on the specific sounding station before applying. The training process, including collecting statistics and training the decision tree, is to customize the model, which  
 245 enables the model to adapt to the data characteristics and QC requirements of different sounding stations, therefore improving the performance.



#### 4.1 Analyzing the moment of sounding termination

The algorithm for identifying the moment of sounding termination based on LDS does not require training. So we conducted the algorithm on the radiosonde data from Fuzhou Station between 2020 and 2022, and compared the results with the manually labelled data. The statistic of deviation between our method and manual labelled results is shown in Figure 5.

The experiment results show that 36.5% of the cases are completely consistent with the manual labelled results. In terms of time, the proportion of cases with time deviation less than or equal to 3 seconds is 74.2%, and the proportion of cases with time deviation less than or equal to 10 seconds is 96.9% (as shown in Figure 5(a)). On the other hand, the comparison in terms of pressure deviation shows that the proportion of cases with pressure deviation within  $[-0.1\text{hPa}, +0.1\text{ hPa}]$  reaches 97.11% (as shown in Figure 5 (b)). The results are highly consistent with manually labeled data, which indicates the high accuracy and reliability of our algorithm on finding the moment of sounding termination.

Through insight into the data, we find that the deviations in sounding termination mainly come from two aspects: (1) The L-band (Type-I) data processing software displays the pressure values rounded to the nearest tenth, which leads to precision loss; (2) Manual quality control is sensitive to changes in adjacent data, but often overlooks some details of data that are far apart.

In summary, the algorithm of identifying the moment of sounding termination based on LDS can output accurate moments of sounding termination. Therefore, this step effectively filters out invalid data during the descent of the balloon.

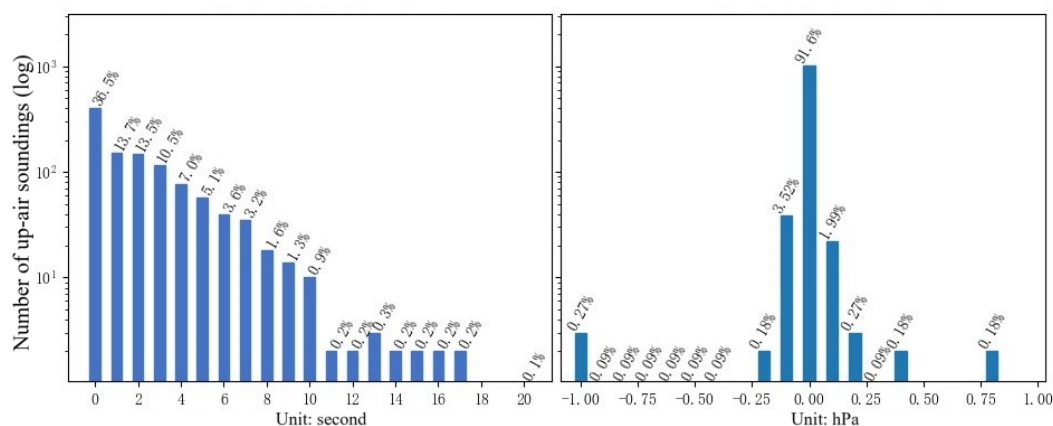


**Figure 5.** Distribution of deviation between automatically determined and manually labelled results from 2020 to 2022 at Fuzhou Station. (a) Distribution on time deviation. (b) Distribution on pressure deviation.

#### 4.2 Result of anomaly analysis based on the Bezier curve fitting

After fitting the temperature, pressure, and relative humidity with the Bezier curve, we calculate  $T\_SCORE$ ,  $P\_SCORE$  and  $H\_SCORE$  to evaluate the deviations. Figure 6 shows the curve of deviation vs anomaly score, and the curve of deviation vs number of labelled anomalies, where the number of labelled anomalies is logarithmically processed. From Figure 6, it can be seen that: (1) Most deviations are small. The labelled anomalies follow a normal distribution and comply with the basic rules



of error distribution. (2) The anomaly scores increase with the absolute values of deviation, indicating that the anomaly score reflects the degree of data deviation, and therefore can be used as an indicator for anomaly determination.

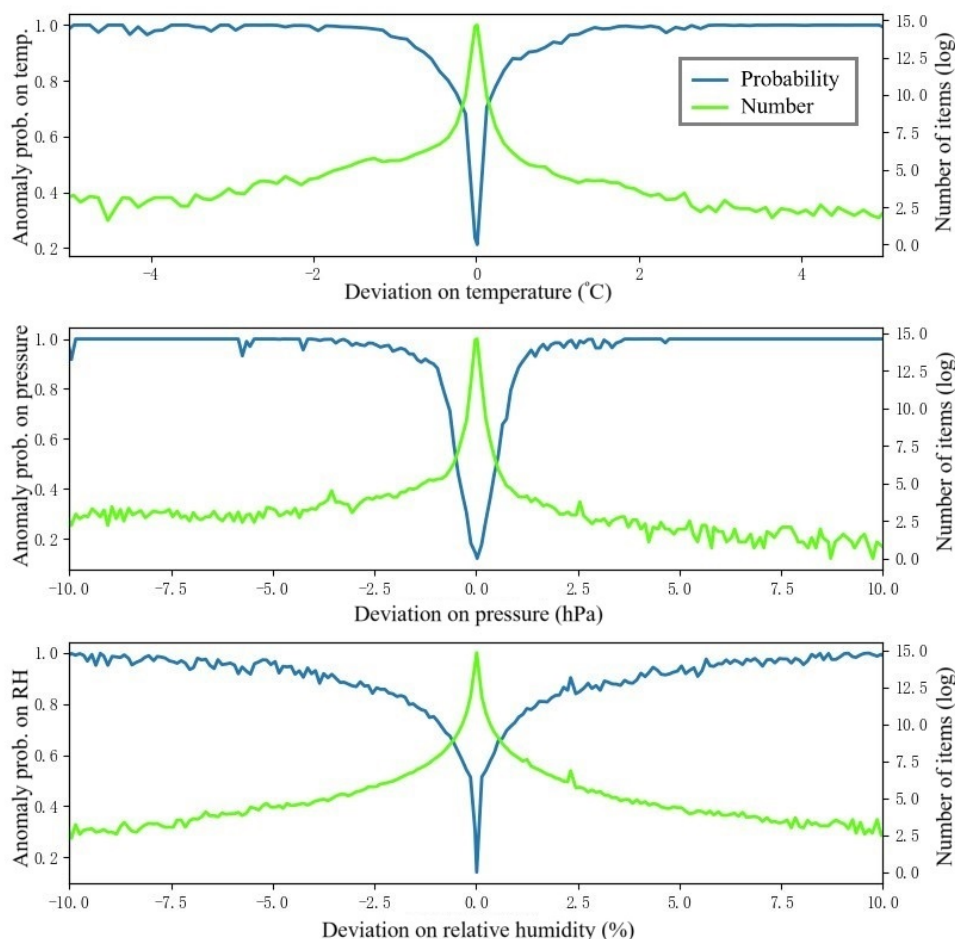


**Figure 6.** Relationship between the fitting deviation of temperature, pressure, and relative humidity and the probability / amount of abnormalities.

### 270 4.3 Performance of our method

Based on  $T\_SCORE$ ,  $P\_SCORE$  and  $H\_SCORE$ , we train CART using data from 2020 and 2021, and validate the result using data from 2022. The performances of our method are shown in Table 2. The statistics of meteorological variables before and after quality control are shown in Table 3.

Table 2 shows that 14.18% of the items are filtered out by our method, while there are 18.56% of the items are filtered out  
275 by manual QC. Based on the manually labeled data, after the stage QC1, the precision of detecting errors is 98.39%, with a recall of 10.14%, indicating that 98.39% of detecting errors overlap with manual labeled errors, and 10.14% manual labeled



errors are detected in stage QC1. Combining the two QC stages, the precision of our algorithm reaches 86.18%, with a recall of 65.86%. Given the experiences of different quality control personnel and the lack of unified quantitative standards, which may lead to inconsistent judgments, the performances fully demonstrate the effectiveness of the method proposed in this paper.

**Table 2.** Performance of our method.

Before QC	Manual QC		Algorithmic QC		QC1		QC1+QC2	
#(items)	#(items)	filtering ratio	#(items)	filtering ratio	precision	recall	precision	recall
4,515,382	3,677,389	18.56%	3,874,929	14.18%	98.39%	10.14%	86.18%	65.86%

280 Table 3 presents a comparison of statistics before and after QC. First, the change rates of temperature and pressure increase after QC. The reason is that our method filters out many stiff values of temperature and pressure, whose change rates are 0. On the contrary, because many jumps in the relative humidity data are excluded, the change rate of relative humidity slightly decreased after QC. In terms of standard deviations of the change rates, the standard deviations of temperature, pressure, and humidity change rates decreased by 97.5%, 99.3%, and 91.7%, indicating a significant reduction in data dispersion, which is  
 285 more consistent with the characteristics of continuous and gradient on temperature, pressure, and relative humidity. Meanwhile, it should be noted that although the filtering ratio is lower than manual QC, the standard deviation is still smaller than manual QC.

**Table 3.** Statistics of meteorological variables before and after quality control.

Weather variable	Mean of change rate			Standard deviation of change rate		
	Before QC	Manual QC	Algorithmic QC	Before QC	Manual QC	Algorithmic QC
Temperature( $^{\circ}C/s$ )	-0.0139	-0.0144	-0.0159	2.6462	0.0664	0.0655
Pressure(hPa/s)	-0.1826	-0.2133	-0.1951	28.1857	0.2096	0.1916
RH(%/s)	-0.0160	-0.0163	-0.0078	2.6092	0.3356	0.2161

#### 4.4 Comparison of percentile profiles

To further validate the effectiveness of our method, the percentile profile (Houchi et al., 2015), was used to inspect the radiosonde data before and after QC. Figure 7 shows the time-varying profiles of temperature, pressure, and relative humidity percentiles, with time as the vertical axis. Figures 8 shows the profiles of temperature and humidity relative to pressure, with pressure as the vertical axis. The percentile thresholds are 0%, 10%, 25%, 50%, 75%, 90%, and 100%.

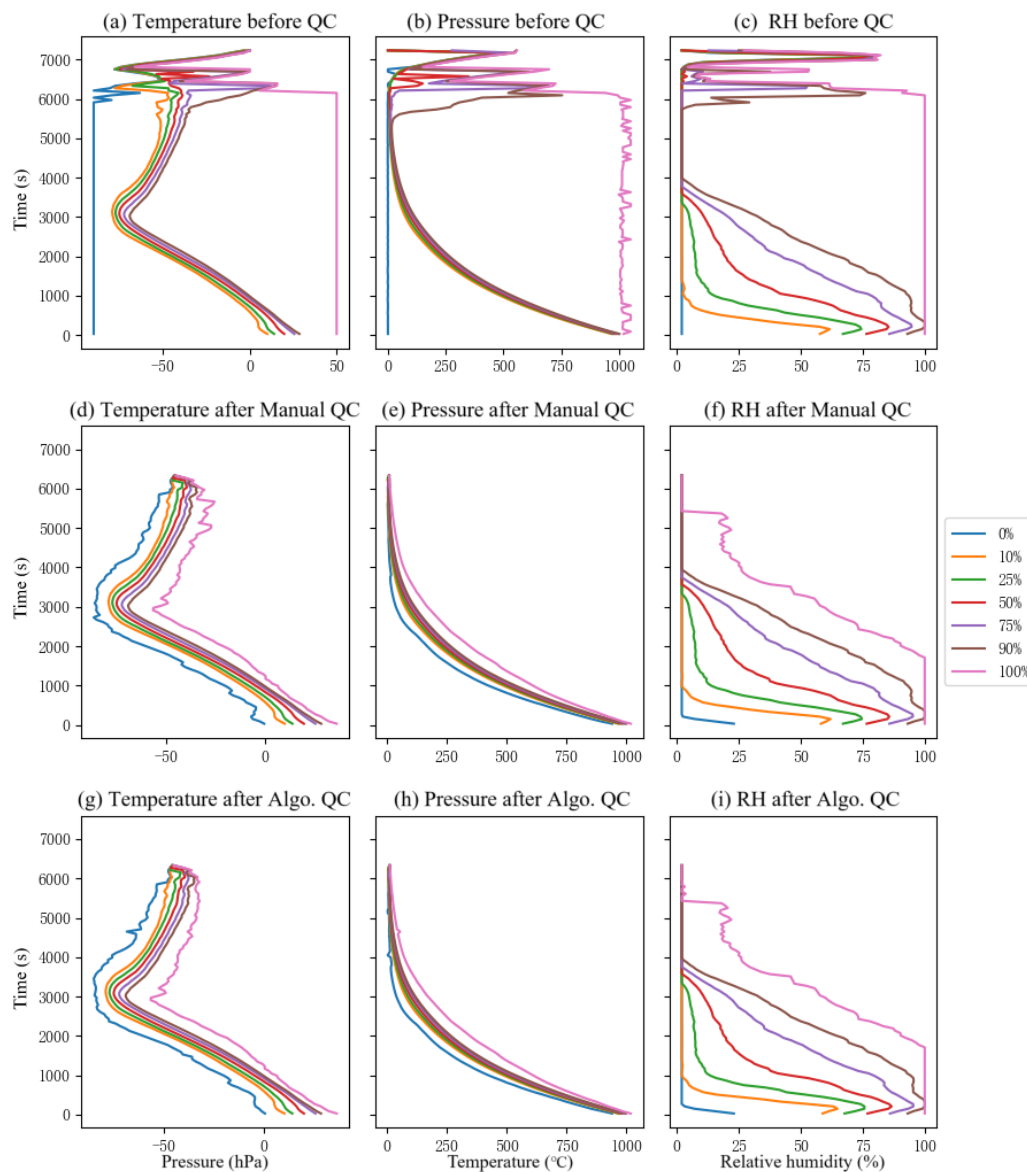


**Figure 7.** Time-varying profiles of temperature, pressure, and relative humidity percentiles before quality control (a, d, g), after manual quality control (b, e, h), and after algorithm quality control using the method proposed in this paper (c, f, i) for second-level radiosonde data.



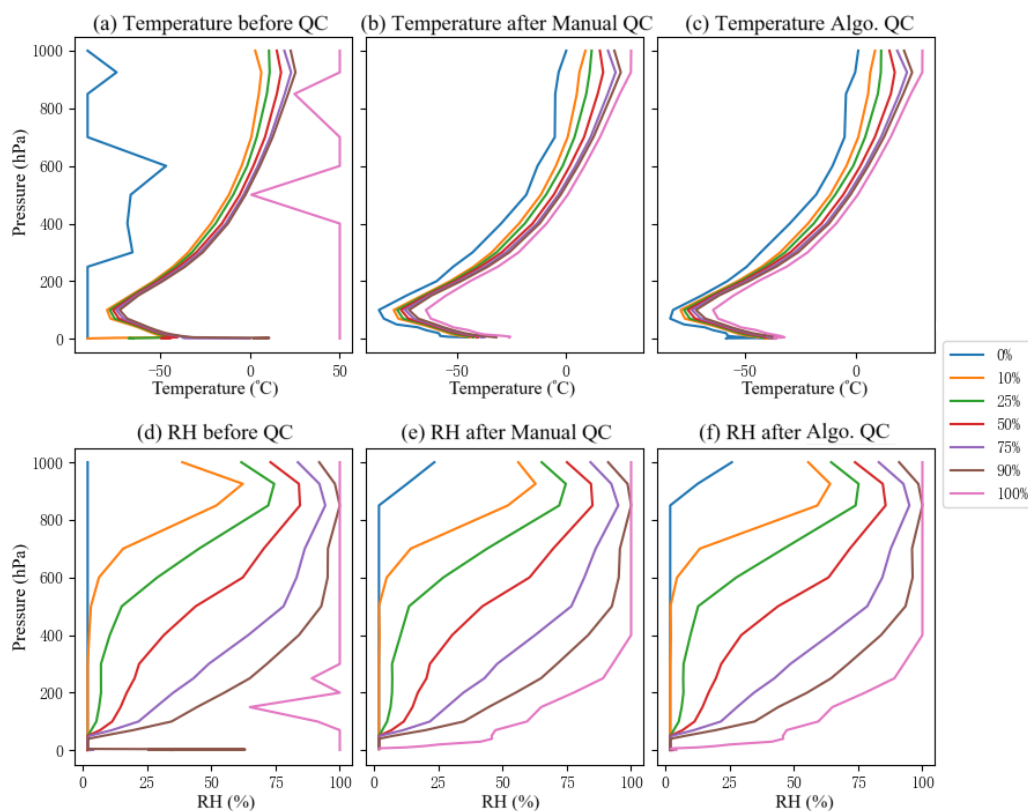


**Figure 8.** Profiles of temperature and humidity relative to pressure before and after quality control for the second-level radiosonde dataset.

From Figures 7 and Figure 8, we find that both the 0% and 100% profiles show many unreasonable situations (inconsistencies and jumps) in the raw data, such as, the monotonic increase of the 90% pressure profile around 5500~6000 seconds (Figure 7(b)), the presence of high humidity in the stratosphere (Figure 7(c)), and the stiff value of the 0% humidity profile at low altitude (>850 hPa) (Figure 8(d)).

After QC by our method, the data distribution and variation trend became more reasonable (as shown in Figure 7(g,h,i), Figure 8(e,f)). Firstly, the jump values in the percentile profiles are eliminated, improving the data consistency. Secondly, by filtering out unreasonable data such as stiff values, the values of each meteorological variable become more reasonable. Thirdly, the removal of abnormalities makes the percentile profile smoother and clearer, and the data distribution near the 50% profile denser, more accurately reflecting the real data distribution. Finally, the radiosonde data accurately reflects some atmospheric phenomena, such as atmospheric inversion layer (0 80 hPa), and the fact that the ascent speed of the balloon is not significantly affected by the decrease in pressure.

By comparing the percentile profiles of algorithm QC results (as shown in Figure 7(g,h,i), Figure 8(e,f)) with the percentile profiles of manual QC results (as shown in Figure 7(d,e,f), Figure 8(c,d)), it can be seen that their shapes are very close, indicating that the difference in QC results between them is small.

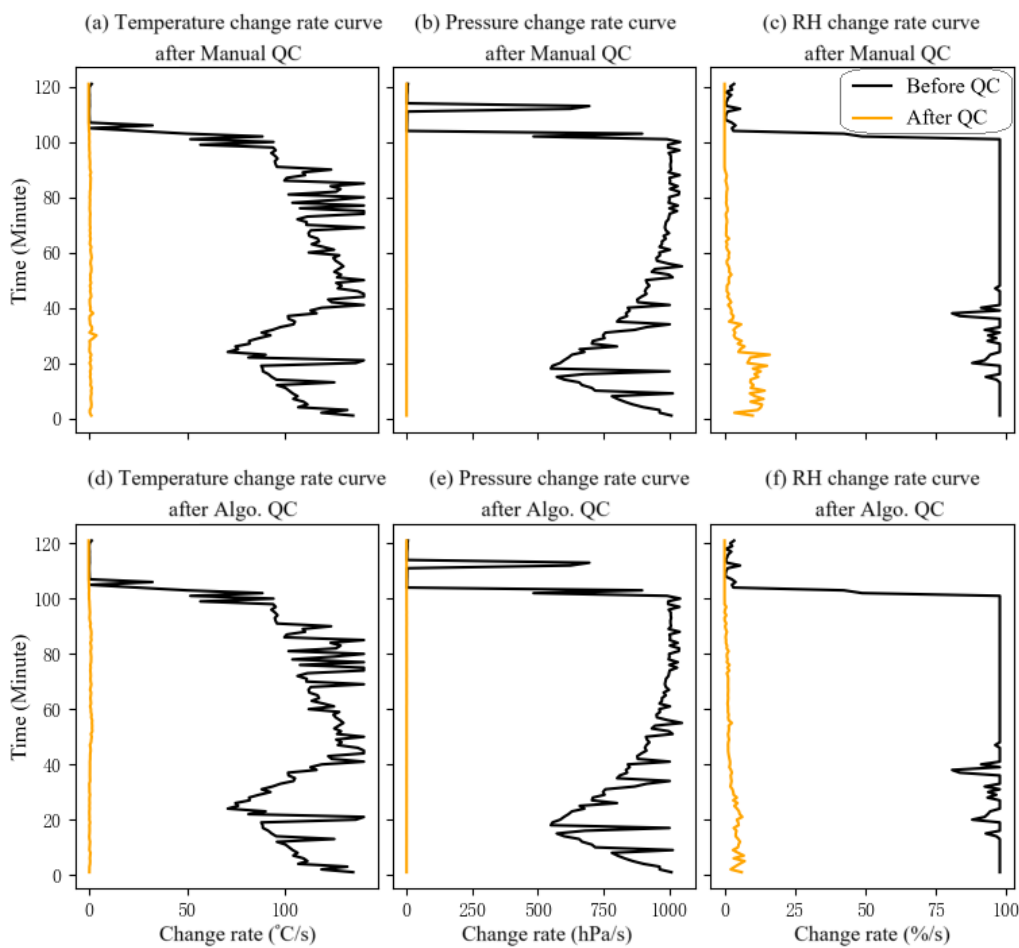


**Figure 9.** Comparison of the maximum value curves of attribute change rates before and after quality control.

In the process of quality control, the maximum change rates of temperature, pressure, and relative humidity can help to determine whether the data series meets the expected changes. Therefore, their evaluation is very important. Figure ?? shows the maximum change rate curves of temperature, pressure, and relative humidity for raw data, manual QC data, and algorithm  
310 QC data. In the raw data, there are a large number of abnormal change rates, manifested as the change rate exceeding the expected range. After QC, the abnormal items are removed. The change rates processed by the algorithm are more reasonable and show a trend of gradual convergence over time, indicating that our method effectively processes the data and makes the change rates more reasonable.

Through analyzing the data in-depth, we found that both algorithmic QC and manual QC achieve effectiveness over pressure  
315 and temperature, following the characteristic of gradually decreasing on pressure and continuous variation on temperature. While values of relative humidity often undergo drastic changes during the process of entering and leaving a cloud, resulting in a wider range of rates of change.



Our method has been applied at 3 sounding stations in Fujian province. Compared with traditional manual quality control methods, the algorithmic QC method proposed in this paper can not only significantly reduce the consumption of human resources, but also help unify the quality control standards for sounding data, effectively improving the quality of radiosonde data.

## 5 Conclusions

Considering the issues with manual quality control, we propose an automatic quality control method for second-level radiosonde data. The method includes two stages: QC1 stage and QC2 stage. In the stage QC1, gross errors are filtered out. In stage QC2, based on the continuity characteristics of 3 meteorological variables, the deviations between Bezier curve fitting and measurement are used for evaluating anomalies. Finally, anomalies are identified through integrating multiple factors.

Based on the dataset from Fuzhou Station from January 1, 2020 to December 31, 2022, we conduct a detailed analysis of the QC effect of the proposed method, and draw the following conclusions: (1) The abnormal items detected in the stage QC1 accounts for 10.14% of the manually labelled errors, with an accuracy of 98.39%, indicating that the QC1 stage can effectively filter out gross errors in the dataset; (2) After the integration analysis in the QC2 stage, the overlap ratio between the abnormal items filtered out using our method and the manually labelled abnormal items reaches 86.18%, demonstrating the feasibility and effectiveness of automatic QC; (3) After being processed by the QC method in this paper, the percentile profiles of temperature, pressure, and relative humidity become more reasonable, and the dispersion of data change rate is significantly reduced. These conclusions verify that the quality control method proposed in this paper can filter out abnormal data and improve the data quality.

The automatic quality control method proposed in this paper provides a feasible QC solution for second-level radiosonde data. The feasibility is verified through experiments. Automatic QC can improve quality control efficiency, unify quality control standards, and ensure the reliability and accuracy of data.

*Data availability.* The data that support the findings of this study are available from China Meteorological Administration. Restrictions apply to the availability of these data, which were used under licence for this study.

*Author contributions.* Conceptualization, BW and SZ; Data curation, HZ and BW; Funding acquisition, HL; Investigation, HL, LC; Methodology, HL, LC and SZ; Project administration, SZ; Software, LC; Validation, LC, WZ, HZ and BW; Visualization, LC; Writing – original draft, LC and HL; Writing – review & editing, HL, YT, HZ and SZ.

*Competing interests.* The authors declare that they have no conflict of interest.



345 *Financial support.* This work was supported by the Project of Fujian Province Science and Technology Plan (2023I0013).



## References

- Agarwal, G. and Sun, Y.: Bivariate Functional Quantile Envelopes With Application to Radiosonde Wind Data, *Technometrics*, 63, 199–211, <https://doi.org/10.1080/00401706.2020.1769734>, 2021.
- Cao, X., Guo, Q., and Yang, R.: Research of rising and falling twice sounding based on long time interval of flat floating, *Chinese Journal of Scientific Instrument*, 40, 198–204, 2019.
- Chen, Z. and Xu, X.: Quality Control of Second by Second Radiosonde Measurements in Sichuan, *Meteorological Science and Technology*, 46, 462–467, 2018.
- Durre, I., Vose, R. S., and Wuertz, D. B.: Robust Automated Quality Assurance of Radiosonde Temperatures, *Journal of Applied Meteorology and Climatology*, 47, 2081 – 2095, <https://doi.org/10.1175/2008JAMC1809.1>, 2008.
- Estévez, J., Gavilán, P., and Giráldez, J.: Guidelines on validation procedures for meteorological data from automatic weather stations, *Journal of Hydrology*, 402, 144–154, <https://doi.org/https://doi.org/10.1016/j.jhydrol.2011.02.031>, 2011.
- Faccani, C., Rabier, F., Fourrié, N., Agustí-Panareda, A., Karbou, F., Moll, P., Lafore, J. P., Nuret, M., Hdidou, F. Z., and Bock, O.: The Impacts of AMMA Radiosonde Data on the French Global Assimilation and Forecast System, *Weather and Forecasting*, 24, 1268–1286, <https://api.semanticscholar.org/CorpusID:123406140>, 2009.
- Gordon, W. J. and Riesenfeld, R. F.: Bernstein-Bézier Methods for the Computer-Aided Design of Free-Form Curves and Surfaces, *J. ACM*, 21, 293–310, <https://doi.org/10.1145/321812.321824>, 1974.
- Graybeal, D. Y., DeGaetano, A. T., and Eggleston, K. L.: Complex Quality Assurance of Historical Hourly Surface Airways Meteorological Data, *Journal of Atmospheric and Oceanic Technology*, 21, 1156 – 1169, [https://doi.org/10.1175/1520-0426\(2004\)021<1156:CQAOHH>2.0.CO;2](https://doi.org/10.1175/1520-0426(2004)021<1156:CQAOHH>2.0.CO;2), 2004.
- Guo, J., Miao, Y., Zhang, Y., Liu, H., Li, Z., Zhang, W., He, J., Lou, M., Yan, Y., Bian, L., and Zhai, P.: The climatology of planetary boundary layer height in China derived from radiosonde and reanalysis data, *Atmospheric Chemistry and Physics*, 16, 13 309–13 319, <https://doi.org/10.5194/acp-16-13309-2016>, 2016.
- Guo, Q., Yang, R., Cheng, K., and Li, C.: Refractive index quality control and comparative analysis of multi-source occultation based on sounding observation, *Journal of Applied Meteorological Science*, 31, 13–26, 2020.
- Guo, Y., Li, Q., and Ding, Y.: The Effect of Artificial Bias on Free Air Temperature Trend Derived from Historical Radiosonde Data in China, *Chinese Journal of Atmospheric Sciences*, 33, 1309–1318, 2009.
- Hao, M., Wang, R., Tian, W., and Wan, X.: The Evaluation and Analysis of Radiosonde Humidity Data Quality in CIMISS and GDAS Database, *Plateau Meteorology*, 39, 1070–1079, 2020.
- Houchi, K., Stoffelen, A., Marseille, G. J., and De Kloe, J.: Comparison of wind and wind shear climatologies derived from high-resolution radiosondes and the ECMWF model, *Journal of Geophysical Research: Atmospheres*, 115, <https://doi.org/https://doi.org/10.1029/2009JD013196>, 2010.
- Houchi, K., Stoffelen, A., Marseille, G.-J., and Kloe, J. D.: Statistical Quality Control of High-Resolution Winds of Different Radiosonde Types for Climatology Analysis, *Journal of Atmospheric and Oceanic Technology*, 32, 1796 – 1812, <https://doi.org/10.1175/JTECH-D-14-00160.1>, 2015.
- Kumar, A. H. and Sunilkumar, S. V.: Assessment of INSAT-3D Retrieved Temperature and Water Vapour With Collocated Radiosonde Measurements Over Indian Region, *IEEE Trans. Geosci. Remote. Sens.*, 58, 4000–4005, <https://doi.org/10.1109/TGRS.2019.2960277>, 2020.



- meteorological administration, C.: Operational specification for routine upper air meteorological observation, China Meteorological Press, Beijing, China, 2010.
- 385 Qian, Y., Ma, X., Guo, Q., Yang, R., and Cao, X.: Error Analysis of Sounding Temperature Data Based on the FNL and GRAPES Analysis Fields, *Meteorological Monthly*, 45, 1464–1475, 2019.
- Su, X., Li, D., and Tang, H.: *A Practical Tutorial in Computer Graphics (4th Edition)*, People's Posts and Telecommunications Press, 2020.
- Tan, J., Chen, B., Wang, W., Yu, W., and Dai, W.: Evaluating Precipitable Water Vapor Products From Fengyun-4A Meteorological Satellite Using Radiosonde, GNSS, and ERA5 Data, *IEEE Trans. Geosci. Remote. Sens.*, 60, 1–12, <https://doi.org/10.1109/TGRS.2022.3146018>,  
390 2022.
- Wang, D., Wang, J., and Tian, W.: Quality Control and Uncertainty Analysis of Return Radiosonde Data, *Chinese Journal of Atmospheric Sciences*, 44, 865–884, 2020.
- Wang, D., Wang, J., and Tian, W.: Research on a Quality Control Method for L Band Second-Level Radiosonde toward Assimilation Applications, *Plateau Meteorology*, 41, 1615–1629, 2022.
- 395 Wang, H., Yang, Z., Yang, D., and Gong, X.: The Method and Application of Automatic Quality Control for Real Time Data from Automatic Weather Stations, *Meteorological Monthly*, 33, 102–109, 2007.
- Xiong, A.: *Research and development technology of ground and upper air climate change data products in China*, China Meteorological Press, 2015.
- Zahumensky, I.: *Guidelines on quality control procedures for data from automatic weather stations*, World Meteorological Organization,  
400 2004.
- Zhai, P.: SOME GROSS ERRORS AND BIASES IN CHINA'S HISTORICAL RADIOSONDE DATA, *Acta Meteorologica Sinica*, 1997, 563–572, 1997.
- Zhang, J., Yang, L., Wang, J., Wang, Y., and Liu, X.: A New Empirical Model of Weighted Mean Temperature Combining ERA5 Reanalysis Data, Radiosonde Data, and TanDEM-X 90m Products over China, *Remote. Sens.*, 16, 855, <https://doi.org/10.3390/RS16050855>, 2024.
- 405 Zhou, Z.: *Machine learning*, Tsinghua University Press, 2016.